Adsorption (2016) 22:371–383
DOI 10.1007/s10450-016-9786-9

Ion-exchange properties of microdispersed sintered detonation nanodiamond

Anton Peristyy[1] · Brett Paull[1] · Pavel N. Nesterenko[1]

Received: 20 January 2016 / Revised: 24 February 2016 / Accepted: 29 February 2016 / Published online: 7 March 2016

Abstract The adsorption of transition metal cations and inorganic anions from aqueous solutions on microdispersed sintered detonation nanodiamond (MSDN) is systematically studied. The selectivity series $Fe^{3+} > Al^{3+} > Cu^{2+} > Mn^{2+} > Zn^{2+} > Cd^{2+} > Co^{2+} > Ni^{2+}$ with maximum adsorption capacity between 2 and 5 μmol g^{-1} is obtained. It is found that anions may significantly contribute to the adsorption of transition metal cations, so the adsorption of CH_3COO^-, Cl^-, $B_4O_7^{2-}$, ClO_4^-, I^-, SO_4^{2-}, $C_2O_4^{2-}$, PO_4^{3-} is also studied. For the first time, dominating adsorption of anions over cations is demonstrated for detonation nanodiamond. The maximum anion-exchange capacity of 50–150 μmol g^{-1} is found for MSDN. Beside of electrostatic interactions, the formation of complexes with hydroxyl groups and interaction with metal impurities contribute to the adsorption of $B_4O_7^{2-}$ and PO_4^{3-}, respectively. Therefore, anion exchange selectivity of MSDN is different from that observed for common anion exchange resins. In all cases, the adsorption on MSDN obeys Langmuir law. The pH effect on the adsorption of SO_4^{2-}, PO_4^{3-} and $B_4O_7^{2-}$ is different from that observed for other anions due to specific interactions.

Keywords Detonation nanodiamond · Adsorption · Metal cations · Inorganic anions · Ion-exchange · Surface

Electronic supplementary material The online version of this article (doi:10.1007/s10450-016-9786-9) contains supplementary material, which is available to authorized users.

✉ Pavel N. Nesterenko
Pavel.Nesterenko@utas.edu.au

[1] Australian Centre for Research on Separation Science, School of Physical Science, University of Tasmania, Private Bag 75, Hobart, TAS 7001, Australia

1 Introduction

The investigations of diamond and diamond containing materials as selective adsorbents for application in solid phase extraction (SPE) and chromatography have intensified significantly during the last decade (Nesterenko and Haddad 2010; Peristyy et al. 2014). This trend is due to superior chemical and mechanical properties of diamond and relatively low cost of production of synthetic diamond. Chemical inertness, excellent mechanical and hydrolytic stability, extraordinary high thermal conductivity in combination with low thermal expansion makes diamond a very promising material for the use in chromatography (Peristyy et al. 2014; Nesterenko and Haddad 2010; Chen et al. 2006). However, there is a lack of information on the adsorption properties of diamond. Especially, this is true for detonation nanodiamond (DND), which has very complex surface chemistry defined by synthesis and purification methods applied during production (Mochalin et al. 2012; Kulakova 2004).

The adsorption of inorganic ions on DND surface is of great importance for various applications as it affects surface charge and, therefore, colloidal stability of its suspensions (Chiganova et al. 1993) and aggregation of DND (Dolenko et al. 2014). Therefore, adsorption of ionic impurities is crucial for DND performance in various applications including galvanic coatings (Chiganova et al. 2013), lubricating compositions (Ivanov et al. 2010), fabrication of electronic devices (Williams 2011) and chromatographic applications (Nesterenko and Haddad 2010; Peristyy et al. 2014; Wiest et al. 2011). Also, ion-exchange properties of DND may be responsible for the negative effects in drug delivery associated with the excessive delivery of sodium ions into the cells and related implications for tumour therapy (Zhu et al. 2012) or for so called "Trojan horse" effect,

connected with intracellular delivery of Cu^{2+}, Cd^{2+}, Cr^{3+} and Ni^{2+} by DND particles and triggering cytotoxicity (Zhu et al. 2015). On the contrary, the controlled adsorption of lanthanides, transition metals and precious metal ions on DND has been also used for the preparation of new useful magnetic and optically active materials for medical diagnostics (Manus et al. 2010), and efficient catalysts (Chiganova et al. 2012).

Undoubtedly, cation-exchange properties of DND are due to the presence of negatively charged carboxylic and phenolic groups at its surface (Paci et al. 2013). For the purified DND the typical value of dzeta potential (ζ) is about −(42–45) mV in suspensions with pH >10 (Mitev et al. 2014a, b). However, higher values of the negative ζ-potential up to −70 mV may be achieved after extensive surface carboxylation. The adsorption of divalent and trivalent metal cations due to complexation with surface carboxylic groups is also possible for DND (Nesterenko et al. 2007; Buchatskaya et al. 2015). At the same time, the preparation of DND samples with high positive values of ζ-potential (50–55 mV) has been also reported by Ozawa et al. (2007) and Petit et al. (2013). In this case, positive ζ-potential is responsible for anion-exchange interactions between this type of DND and inorganic anions (Sakurai et al. 2006).

The number of publications on systematic investigation of adsorption of inorganic ions by DND is rather limited and non-informative. As a rule, the authors of these publications reported only values of adsorption capacity for various cations. For example, Bogatyreva et al. (2008a, b) reported the adsorption capacities of 0.20 and 0.16 mmol g^{-1} for Fe^{3+} and Ni^{2+}, respectively, for the DND sample with specific surface area $S = 172$ m^2 g^{-1}. The adsorption capacities of 0.49, 0.44, 0.30 and 0.10 mmol g^{-1} are reported for DND (no presented data on surface area) by Zhu et al. (2015) for Cr^{3+}, Cu^{2+}, Ni^{2+} and Cd^{2+}, respectively. Significantly higher adsorption capacity of 3.37 mmol g^{-1} was measured for Al^{3+} by Chiganova et al. (1993), which can be explained by hydrolysis of aluminium salt and precipitation of aluminium hydroxide under experimental conditions. Chukhaeva and Cheburina (2000) measured adsorption capacity for Cs^+ for 12 DND samples produced using different purification technologies. The obtained values varied from 0.005 to 0.7 mmol g^{-1}, while the maximum value was obtained for DND sample purified with chromic anhydride. Nesterenko and co-authors reported adsorption capacity 2.0 mmol g^{-1} for Na^+ (Mitev et al. 2014a, b) by using direct ICP-MS analysis for determination of elemental impurities in DND (Mitev et al. 2013).

These capacities are in a good agreement with the reported data on surface concentration of acidic carboxylic functional groups in DND. The values of 0.15–0.81 COOH groups per nm^2 and up to 0.20 lactone groups per nm^2 (Schmidlin et al. 2012) are obtained by Boehm titration, while acid–base potentiometric titration revealed the presence of 1.3–1.4 carboxylic groups per nm^2 (Chiganova et al. 2012; Nguyen et al. 2007; Mitev et al. 2014a, b). Assuming that DND particles have a spherical shape of average diameter $d_p = 4.5$ nm with density $\rho = 3.5$ g cm^{-3}, the maximum value of specific surface area ($S = 6/\rho d_p$) could be as high as 380 m^2 g^{-1}, and the corresponding ion-exchange capacity due to presented in DND carboxylic groups could be as high as 0.89 mmol g^{-1}. It should be noted that this value of ion-exchange capacity is comparable with that reported for commercially available cation-exchange resins (Haddad et al. 2008).

There is also communication on adsorption of inorganic anions by DND. Sakurai et al. investigated adsorption of AsO_3^{3-}, AsO_4^{3-}, $Cr_2O_7^{2-}$, ReO_4^{2-}, SeO_3^{2-}, SeO_4^{2-}, MoO_4^{2-}, and WO_4^{2-} using DND treated by ball milling and containing 0.4 % of Zr. The quantitative adsorption of WO_4^{2-} from aqueous solution with maximum capacity of 0.064 mmol g^{-1} was found, while only partial adsorption was noted for AsO_4^{3-}, $Cr_2O_7^{2-}$ and MoO_4^{2-} (Sakurai et al. 2006) with adsorption capacities of 2.4, 3.0 and 6.5 μmol g^{-1}, respectively. It was proposed that the positive surface charge of this type of DND ($\zeta = 55$ mV at pH = 6) and anion uptake could be associated with the presence of protonated primary amino groups at the DND surface. However, no adsorption of Cu^{2+} owing to complexation with primary amino groups was noted at these conditions.

Interestingly, despite the presence of negatively charged functional groups at the surface, the capability of DND to adsorb anions has been also demonstrated. For example, adsorption of anionic complexes $AuCl_4^-$ and $[Rh(H_2O)_{6-n}Cl_n]^{3-n}$ ($n = 4, 5$) was studied by Skorik et al. (2011), and maximum adsorption capacity of 1.1 mmol g^{-1} was found for the latter complex.

Several mechanisms have been proposed for the retention of cations and anions on the surface of diamond, but the majority of them are inconclusive and unable to explain important experimental details. For example, a possibility of co-joint adsorption of cations and anions on polyampholyte surface of DND has not been considered as an option. Therefore, the goal of this work is investigation of adsorption of metal cations and inorganic anions on MSDN with the focus on zwitter-ionic properties of DND.

2 Experimental

2.1 Materials and reagents

All adsorption experiments were carried out using additionally fractionated MSDN sample (PDD 3–6) purchased from ALIT Co. (Kiev, Ukraine). The preparation, properties of MSDN particles and chromatographic performance

have been described in the literature (Bogatyreva et al. 2000; Yushin et al. 2005; Fedyanina and Nesterenko 2010, 2011; Nesterenko and Fedyanina 2010). Before the use MSDN was purified by washing with 5 M HNO_3 in order to remove metal impurities, followed by washing with 1 M NaOH to remove adsorbed anions, and then again with 5 M HNO_3 to ensure all surface groups are protonated. Finally, the excess of HNO_3 was removed by flushing MSDN with DIW until the pH of washings was in the range 4.5–5.0.

The following salts $MnSO_4$, $NaClO_4$ (all from AJAX Chemicals, Scoresby, VIC, Australia), $Zn(NO_3)_2$, $CoSO_4$, $CuCl_2$, $CuSO_4$, Na_2SO_4, $Cu(NO_3)_2$, $Na_2C_2O_4$, NaCl (Sigma-Aldrich, Castle Hill, NSW, Australia), $Cd(NO_3)_2$, $NiSO_4$, $Al(NO_3)_3$, Na_3PO_4, NaI, $Fe(NO_3)_3$ (99 %, all from VWR International, Murarrie, QLD, Australia) were used for the preparation of stock solutions of cations and anions. Solutions of hexamine, $Na_2B_4O_7$, CH_3COOH were used as pH buffers, while concentrated HNO_3, H_2SO_4 (99 %, all from Chem-Supply, Gillman, SA, Australia), H_3PO_4 (99 %, all from Univar, Ingleburn, NSW, Australia) and NaOH (99 % Scharlau, Sentmenat, Barcelona, Spain) were used for the pH adjustment. Deionised water (DIW) was obtained from a Milli-Q system (Millipore, USA) and used for the preparation of all solutions.

For the adsorption experiments, 0.2 g of MSDN and 10 mL of the ion-containing solution of required concentration and adjusted pH were placed in polypropylene test tubes. After shaking for at least 30 min (shorter times were applied in kinetics study of adsorption), the test tubes were centrifuged, and the supernatant was collected and filtered through a membrane filter (pore size 0.45 μm). The determination of ion concentrations in supernatant was performed using either ion chromatography (IC) or spectrophotometrically with *o*-cresolphtalein (99 %, Sigma-Aldrich, Castle Hill, NSW, Australia), 4-(2-pyridylazo)resorcinol (PAR) (98 %, Kodak, Rochester, NY, USA), or chromazurol S (85 %, Riedel-de-Haën, Sigma-Aldrich, Seelze, Germany). 0.1 M HNO_3 was used to desorb metal cations from MSDN.

2.2 Instrumentation

A Nanoseries zetasizer Model Zen3600 (Malvern Instruments, Malvern, Worcestershire, UK) was used for ζ-potential measurements. The Smoluchowski approximation for large particle sizes (1–2 μm) and high ionic strengths (>100 mM) was used according to Hunter (1981). SEM images of MSDN particles were obtained with Hitachi SU-70 (Hitachi Ltd., Chiyoda, Tokyo, TKY, Japan) field emission scanning electron microscope and 1.5 keV electron beam. All samples were platinum-sputtered prior to analysis. BET surface area measurements and porous structure of MSND were measured by adsorption of nitrogen at low temperatures using Micromeritics TriStar II analyser (Norcross, GA, USA).

FTIR spectra of MSDN were obtained using Bruker MPA spectrometer (Billerica, MA, USA). Prior to measuring FTIR spectra, MSDN powder was dried overnight in a vacuum oven at 100 °C and 0.4 atm. Potassium bromide tablets containing 5 % w/w of MSDN were used as samples.

2.3 Experiments on adsorption of ions

2.3.1 Determination of metal cations

IC system comprising AS50 autosampler, IP25 isocratic pump, and AD25 photometric detector (all from Thermo Scientific, Sunnyvale, CA, USA) was used for the determination of the transition metal cations. IonPac CS16 column (250 mm × 3.0 mm ID) was used for the determination of metal ions (Zn^{2+}, Mn^{2+}, Co^{2+}, Ni^{2+}, Cd^{2+}, Cu^{2+}, Fe^{3+}) with 0.1 M HNO_3 as eluent at flow rate of 0.36 mL min^{-1}. A 1.0×10^{-4} M solution of PAR in 0.1 M sodium tetraborate buffer (pH 9.18) was used as post column reagent for the photometric detection of metals at 490 nm. Similarly, 1.0×10^{-4} M solution of chromazurol-S in 0.1 M hexamine buffer (pH = 6.0) was used for the photometric detection of Al^{3+} at 545 nm using UV–Vis spectrophotometer Metertech SP-8001 (Nankang, Taipei, Taiwan).

2.3.2 Determination of inorganic anions

ICS-2000 ion chromatograph (Thermo Scientific, Sunnyvale, CA, USA) equipped with an AS50 autosampler, conductivity detector and IonPac AS19 column (250 mm × 4.0 mm ID) was used for the determination of inorganic anions. 40 mM KOH eluent was generated by eluent generator EGC-II and used for the separation of NO_3^-, SO_4^{2-}, ClO_4^-, Cl^-, I^-, and PO_4^{3-} at 30 °C and 1 mL min^{-1} flow rate. $B_4O_7^{2-}$ and $C_2O_4^{2-}$ were quantified using ion-exclusion IC mode with an IonPac ICE-AS6 column (250 mm × 9.0 mm ID) and 10 mM H_2SO_4 eluent at 1 mL min^{-1}.

2.3.3 Boehm titration

Acid–base potentiometric titration was accomplished using Metrohm 809 Titrando autotitrator with Tiamo 1.2 software (MEP, Mitcham, VIC, Australia). Vent capsule filled with Lecosorb $NaOH/SiO_2$ adsorbent (Leco Corporation, St. Joseph, MI, USA) was attached to titrant container in order to prevent CO_2 uptake by NaOH titrants. Prior to titration, all acidic groups at the surface of MSDN were protonated by consecutive washing with 5 mM HCl and DIW, and drying at 100 °C. 4.8 mM HCl solution used in titration experiments was normalised with 10 mM standard

solution of potassium hydrogen phthalate prepared by dissolving a precisely weighted amount of anhydrous salt in water using volumetric flask. 0.5 g of dried MSDN was placed in three 50 mL polypropylene vials and 20 mL of solutions of NaOH, $NaHCO_3$ or Na_2CO_3 ($\sim$10 mM) were added according to the original work of Boehm (1994). Vials were kept for 1 h being sporadically shaken. After centrifugation the supernatant was collected and filtered through 0.22 μm pore size Nylon filter. Aliquots of 5 mL of filtrates were titrated with 4.8 mM HCl solution. Both initial (C_0) and equilibrium concentrations (C_{eq}) of NaOH, $NaHCO_3$ and Na_2CO_3 were determined by titration. Uptakes of NaOH, $NaHCO_3$ or Na_2CO_3 (U, mmol g^{-1}), which indicate the concentrations of acidic groups (C) of different acidity at the surface of MSDN, were calculated as following:

$$U = \frac{V_{base} \times (C_0 - C_{eq})}{m} \quad (1)$$

where V_{base} is the volume of the added alkaline solution (20 mL) and m is the mass of the titrated MSDN (0.5 g).

2.4 Adsorption isotherms

Solutions of increasing concentrations (0–100 μmol mL^{-1}) were used to study the adsorption of ions on MSDN (0.2 g) from solutions of constant volume (5 mL). Adsorption (A, μmol g^{-1}) was calculated as follows:

$$A = \frac{(C_0 - C_{eq}) \cdot V}{m} \quad (2)$$

where C_0 and C are original and equilibrium concentrations (μmol mL^{-1}) of the ion, V is volume of solution (mL) and m is weight (g) of MSDN. Adsorption values (μmol g^{-1}) were plotted *versus* equilibrium concentration of ion after adsorption.

Langmuir and Freundlich models (Eqs. 3 and 4, respectively) were applied to describe the adsorption isotherms:

$$A = \frac{A_{\max} \cdot K_L \cdot C}{1 + K_L \cdot C} \quad (3)$$

where A_{max} is the limit of adsorption achieved by increasing concentration C and K_L is coefficient equal to the slope of adsorption isotherm at low ion concentrations. K_L is also proportional to the distribution coefficient (K_D). Freundlich isotherm of adsorption is described as follows:

$$A = K_F \cdot C^{1/n} \quad (4)$$

where n and K_F are constants. Correlation factors (R^2) between the experimental and simulated isotherms were calculated in order to check which model fits better the experimental data.

3 Results and discussion

3.1 Fractionation, purification and porous structure of MSDN

The original batch of MSDN contained particles with broad distribution on size from 10 nm to 30–40 μm. The presence of fine particles of size <200 nm may cause some problems in handling MSDN during experiments and could decrease the accuracy of the results. Therefore, the fine particles were removed from the original batch of MSDN by repetitive sedimentation from isopropanol. SEM image of finally isolated fraction (see Fig. 1) shows the presence of particles with the sizes between 0.5 and 20 μm. Each of these particles is composed of nanoparticles of size 5–30 nm.

According to producer data (Mitev et al. 2014a, b) the supplied MSDN contained 12.59 mg g^{-1} (or 1.259 mass%) of elemental impurities (Ca, Cr, Ni, Mn, Sn, Fe, Si and others) including 4.27 mg of Fe and 1.43 mg of Si per gram, respectively. The presence of elemental impurities in MSDN could effect on adsorption data for selected ions, so fractionated MSDN particles were additionally purified as described in Sect. 2.1. The accurate control of impurities in purified MSDN was performed using inductively coupled plasma – mass spectrometry (ICP-MS) as described (Mitev et al. 2013). The results of ICP-MS analysis of MSDN after purification (see Sect. 2.1) showed the significant decrease in amount of metal impurities including 556.5 μg g^{-1} of Cr, 169.1 μg g^{-1} of Fe, 141.8 μg g^{-1} of Cu, 111.5 μg g^{-1} of Al, 29.6 μg g^{-1} of Zn, 18.8 μg g^{-1} of Ni, 3.0 μg g^{-1} of Mn and others (Mitev et al. 2014a, b). Obviously, these amounts of impurities are due to metals entrapped into MSDN matrix during detonation synthesis, and therefore they should not influence the results on adsorption of ions.

The isotherm of nitrogen adsorption at low temperatures has characteristic Type IV shape with hysteresis (Fig. 2a), which is typical for mesoporous adsorbents. Brunauer–Emmett–Teller (BET) and Barrett–Joyner–Halenda (BJH) methods were used for the evaluation of surface area (S) and pore size (D_{pore}) and pore volume of MSDN. The obtained value of surface area 191 m^2 g^{-1} was slightly higher than 153 m^2 g^{-1} reported by the manufacturer (Bogatyreva et al. 2008a, b). As shown in Fig. 2b, the major pores have diameter about 4.0 nm, but significant amount of smaller mesopores and micropores is also present.

3.2 Surface characterisation

3.2.1 Surface chemistry

According to the literature, various oxygen containing functional groups are present at the surface of DND

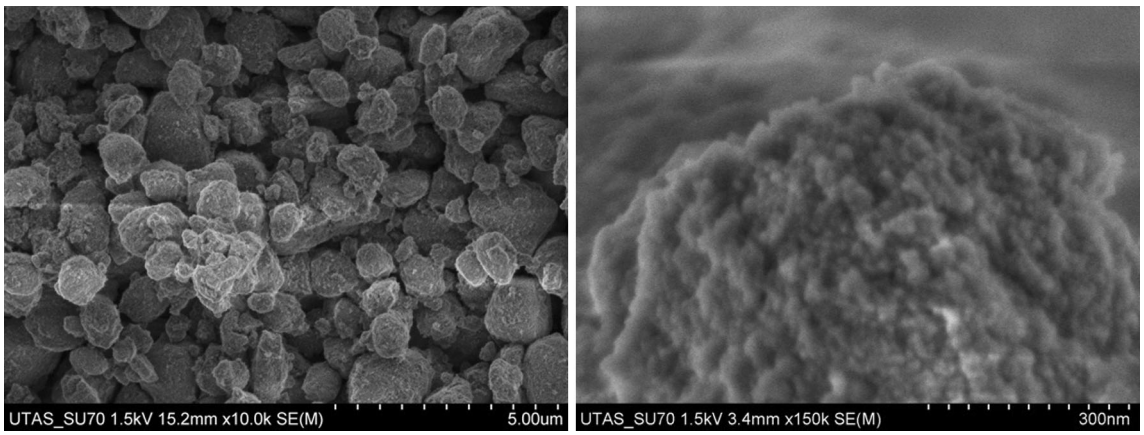

Fig. 1 SEM images of MSDN (see Sect. 2.2 for details)

(Schmidlin et al. 2012; Kulakova 2004; Paci et al. 2013; Nesterenko and Fedyanina 2010) including carboxyls, carbonyls, hydroxyls and lactones. To evaluate the amount of these functional groups the FTIR spectrum of MSDN was obtained (Fig. 3).The broad absorption band at 3000–3600 cm^{-1} corresponds to O–H stretching mode, and can be attributed to adsorbed water, hydroxyl groups and the OH of the carboxyl groups. The related shoulder at 2890–2970 cm^{-1} can be assign to C–H symmetric and asymmetric stretches. The characteristic band at 1735 cm^{-1} is due to the C=O stretching of the carbonyl. The band at 1000–1320 cm^{-1} is related to C–O stretches in the hydroxyl groups. The spectrum confirms the presence of oxygen-containing functional groups in MSDN and indicates the hydrophilic character of this material. Overall, the observed FTIR spectrum is similar to reported previously for MSDN (Nesterenko and Fedyanina 2010).

3.2.2 *Surface charge*

As discussed in Sect. 1, ζ-potential of DND may vary in the range from −70 to +55 mV depending on the type of applied purification, disaggregation and modification (Paci et al. 2013; Gibson et al. 2009; Petit et al. 2013; Ozawa et al. 2007). The occurrence of negative ζ-potentials in alkaline conditions is associated with the presence of dissociated hydroxyl- and carboxyl groups, but the reasons for the positive ζ-potential can be more complex. The simple explanation is based on the presence of protonated nitrogen-containing functionalities. However, neither N–H nor

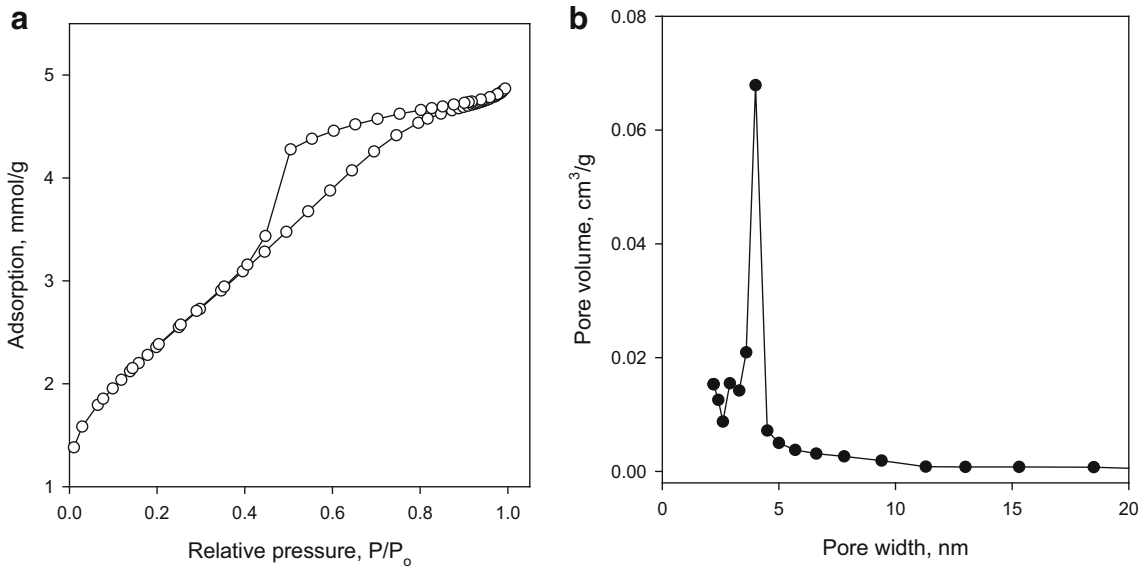

Fig. 2 Adsorption isotherm of nitrogen (**a**) and dependence of pore volume on pore width (**b**) for fractionated MSDN sample

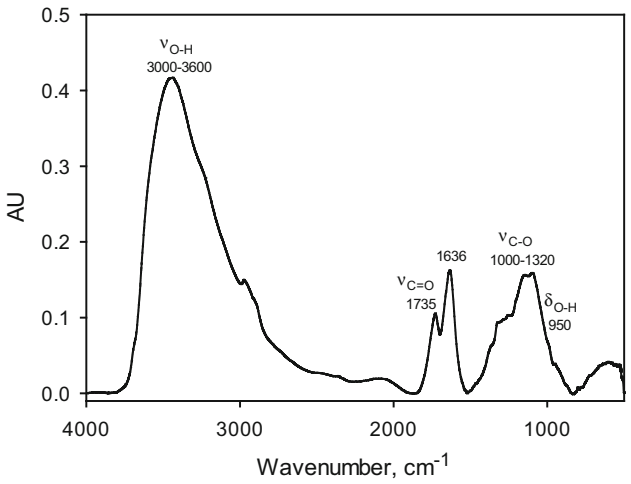

Fig. 3 FTIR spectrum of purified MSDN

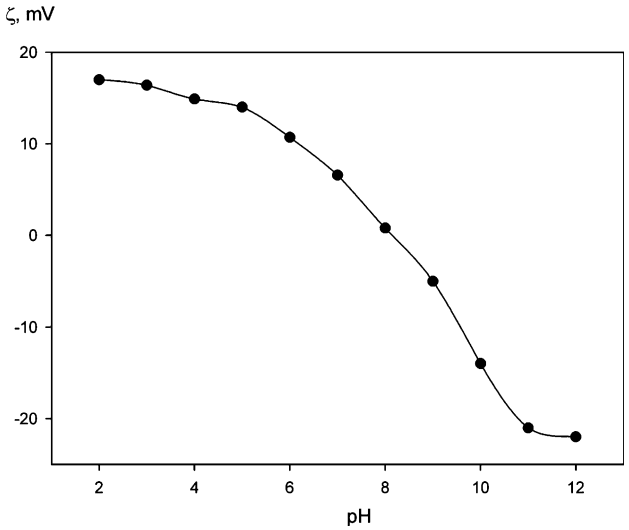

Fig. 4 pH profile of ζ-potential for MSDN. Measured for 0.1 mg mL^{-1} aqueous suspension of MSDN ($\mu = 0.01$ M). pH adjusted with either NaOH or HNO_3 1 M solutions

C–N related bands can be found at detectable levels in FTIR spectrum of MSDN (Fig. 3). Another possible explanation is connected with the presence of sp^2-carbon layer with various functional groups at the external surface of DND (Mochalin et al. 2012). Therefore, the positive ζ-potential can be attributed to the protonation of pyrone, chromene and phenol functional groups at graphitic surface of MSDN (Paci et al. 2013). It should be noted that Penner and Nesterenko (2000) have observed similar effect for hyper crosslinked polystyrene, when protonation of carbonyl groups was responsible for anion-exchange of inorganic anions. The maximum of anion-exchange capacity was achieved at pH 2. Finally, the presence of positive net charge at (100) facets and neutral or negative net charges at (111) facets in diamond nanoparticles was proposed by Chang et al. (2011). However, no clear experimental proofs were provided for the last hypothesis.

Figure 4 presents the dependence of ζ-potential on pH of aqueous suspension for the prepared MSDN sample. At pH 2 MSDN surface has a maximum positive ζ-potential of +17 mV. This value gradually reduces with the increase in pH, with an isoelectric point observed at pH 8.0. The further rise in pH increases negative ζ-potential of MSDN surface up to −23 mV at pH 12. Typical value of negative ζ-potential for untreated DND with fully dissociated functional groups is about 30–35 mV, which is slightly higher than that measured for MSDN sample.

3.3 Adsorption of ions

Very little attention has been paid to the investigation of adsorption mechanism for inorganic ions on DND in the past. Due to the presence of both negative and positive charges at the surface, MSDN may exhibit zwitter-ionic properties, so the adsorption of both anions and cations was studied in this work. The adsorption properties of MSDN were investigated using different buffers, pH of solutions, solute concentrations and sample volumes.

3.3.1 Metal cations

3.3.1.1 pH dependence and adsorption selectivity As shown in Fig. 5, MSDN adsorbs metals cations from 0.05 M sodium phosphate buffer over pH range from 1 to 6 and the following affinity row $Al^{3+} > Fe^{3+} > Cu^{2+} > Mn^{2+} > Zn^{2+} > Co^{2+} > Ni^{2+} > Cd^{2+}$ was obtained. This selectivity is similar to $Fe^{3+} > Ni^{2+} > Cr^{3+} > Pb^{2+} > Cd^{2+}$ reported by Bogatyreva et al. (2008a, b; 2010a, b). Surprisingly, the adsorption of metal cations takes place in acidic solutions with pH <7 despite the expected repulsion of cations from positively charged surface as shown in Fig. 4. The obtained selectivity order differs from the selectivity series $Cu^{2+} > Zn^{2+} > Cd^{2+} > Ni^{2+} > Mn^{2+}$ and $Cu^{2+} > Ni^{2+} > Co^{2+} > Zn^{2+} > Mn^{2+}$ previously reported for common carboxylic cation exchangers (Hubicki and Kolodynska 2015) and oxidised active carbon, respectively (Strelko and Malik 2002). This difference can be explained by dual nature of adsorption mechanism for metal cations on MSDN (Nesterenko et al. 2007). First option includes a combination of electrostatic interactions between negatively charged carboxyls and protonated carbonyls located at MSDN surface and inorganic cations and anions from the solution. The other option is coordination of metal cations with either two carboxylic groups or with one carboxylic and one hydroxyl group located at the surface in a close proximity, when the formation of stable surface complexes is possible due to the chelation

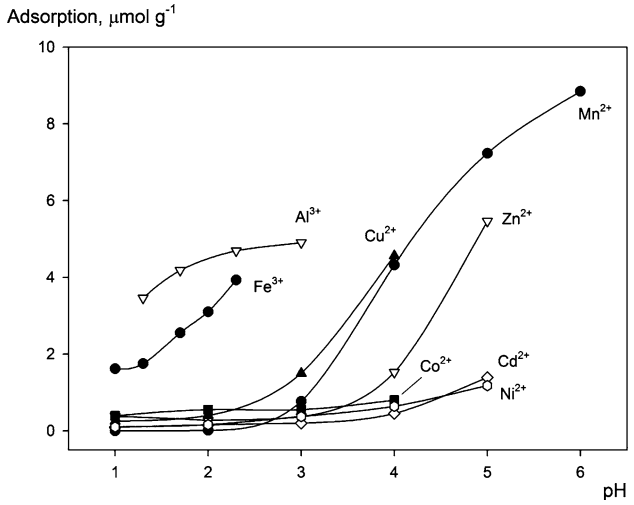

Fig. 5 Adsorption of various metals on MSDN versus pH of solutions. Sample volume: 10 mL of 10 μg mL^{-1} of corresponding salts. Solutions in 0.05 M sodium phosphate buffer and HNO_3 solutions of varied concentration were used for pH >3.0 and pH ≤3.0, respectively

effect (Nesterenko et al. 2007). Also, it was found that the presence of sp^2-carbon at the surface of DND has a strong influence on the adsorption of transition metals (Bogatyreva et al. 2010a, b). The maximum adsorption of Fe^{3+}, Ni^{2+}, Cr^{3+}, Pb^{2+}, and Cd^{2+} was obtained for DND with 80:20 ratio of diamond core to sp^2-carbon shell. Additionally, the hydrophobicity of the DND has a strong effect on adsorption (Bogatyreva et al. 2010a, b), which is relevant to the concentration of polar carboxyl and hydroxyl- groups at the surface.

As expected, MSDN demonstrated a higher affinity towards triple charged Fe^{3+} and Al^{3+}, which can be adsorbed from acidic solutions with pH from 1 to 3 (Fig. 5). This is in agreement with the results on investigation of adsorption of triple charged lanthanides and actinides cations on DND (Watanabe and Kimura 2012). In this pH range the surface of MSDN is positively charged (see Fig. 4), and the adsorption of Fe^{3+} and Al^{3+} can be only due to the formation of relatively stable complexes with oxygen-containing functional groups at the surface (Nesterenko and Jones 2007).

High affinity of MSDN towards Cu^{2+} and Mn^{2+} was also noted (Fig. 5) at pH >3. It is known that Cu^{2+} can form stable octahedral complexes with carboxylic groups presented on the surface of oxidised active carbon (Strelko and Malik 2002) or sp^2 carbon coated MSDN (Shames et al. 2010). However, the reason for the high affinity of MSDN towards Mn^{2+} is not completely clear. Probably, this is due to co-adsorption of Mn^{2+} and phosphate ions from phosphate buffer used in this set of experiments.

For the rest of cations (Zn^{2+}, Ni^{2+}, Co^{2+} and Cd^{2+}) the adsorption increased gradually with the increase of pH from 3 to 5, while substantial adsorption was observed only for Zn^{2+}. A weak adsorption of Ni^{2+}, Co^{2+} and Cd^{2+} (~1 μg g^{-1}) by MSDN was noted at pH >4.0. It should be underlined that the adsorption of metal cations at pH above 5–6 may be affected by hydrolysis and precipitation of insoluble phosphates or hydroxides, therefore the adsorption was not studied at pH >6, depending on the cation. Fig. 1S in supporting information provides the solubility product constants (K_{sp}, see Table 1S in supplementary) for the corresponding metal phosphates (Cu^{2+}, Cd^{2+}, Co^{2+}, Zn^{2+}, Ni^{2+} and Mn^{2+}) and hydroxides (Al^{3+}, Fe^{3+}) and calculated pH values at which precipitation of the corresponding species begins under given conditions (metal concentration 10 mg L^{-1}, 0.05 M phosphate buffer). It should be noted that adsorption of trivalent metals at pH 1–3 from diluted nitric acid solutions.

3.3.1.2 Adsorption capacity The adsorption capacity of MSDN depends on the type and surface concentrations of various groups such as carboxy-, hydroxy-, carbonyls and others. Boehm titration is used for the determination of functional groups in carbonaceous adsorbents according to their acidity by reaction with HCl, sodium bicarbonate, sodium carbonate and sodium hydroxide. The results of Boehm titration of MSDN, diamond of static synthesis at high temperature and high pressure, activated carbon and carbon black are presented in Table 1. The relatively high density of 0.45–0.56 acidic functional groups per nm^2 of the surface of different types of diamond was obtained, which is 3–10 times higher than values reported for activated carbon and carbon black (Kalijadis et al. 2011). The total ion-exchange capacity of MSDN (0.177 mmol g^{-1}) is comparable with the capacity of 0.4–1.0 mmol g^{-1} for commercial ion-exchange resins (Haddad et al. 2008). As above noted the highest adsorption capacity of DND measured for caesium was 0.7 mmol g^{-1} (Chukhaeva and Cheburina 2000), but an absolute maximum of ion-exchange capacity of 2.0 mmol g^{-1} was reported for DND after the treatment with concentrated sodium carbonate solution (Mitev et al. 2014a, b).

In the case of adsorption of transition metals, the highest value of adsorption capacity of 9 μmol g^{-1} was observed for Mn^{2+}. This value is significantly less than the values of 200–300 μmol g^{-1} reported for activated carbon (Strelko and Malik 2002). However, it should be taken into account, that the surface area of MSDN used in this work is 191 m^2 g^{-1}, which is approximately four times less than the values for activated carbon (850 m^2 g^{-1}) and carbon black (up to 1500 m^2 g^{-1}) as presented in the Table 1.

It is likely that the diamond surface possesses diphilic character and adsorption of both cations and anions can occur (Dolenko et al. 2014; Sakurai et al. 2006; Nesterenko et al. 2007). However, the direct titration with HCl shows the presence of only minor anion-exchange capacity (Table 1).

Table 1 Experimental and literature data for Boehm titration of various carbonaceous materials

Material	S (m^2 g^{-1})	U (μmol g^{-1})				C (group nm^{-2})	Ref.
		NaOH	Na_2CO_3	$NaHCO_3$	HCl		
MSDN	191	177	132	117	6.9	0.56	This work
DND	272	203	140	69	5.3	0.45	This work and Mitev et al. (2014a, b)
HPHT diamond	5.1	4.59	3.27	2.39	0.43	0.54	This work and Peristyy et al. (2015)
Activated carbon	960	282	72	29	–	0.18	Kalijadis et al. (2011)
Carbon black	1500	146	38	14	–	0.06	Goertzen et al. (2010)

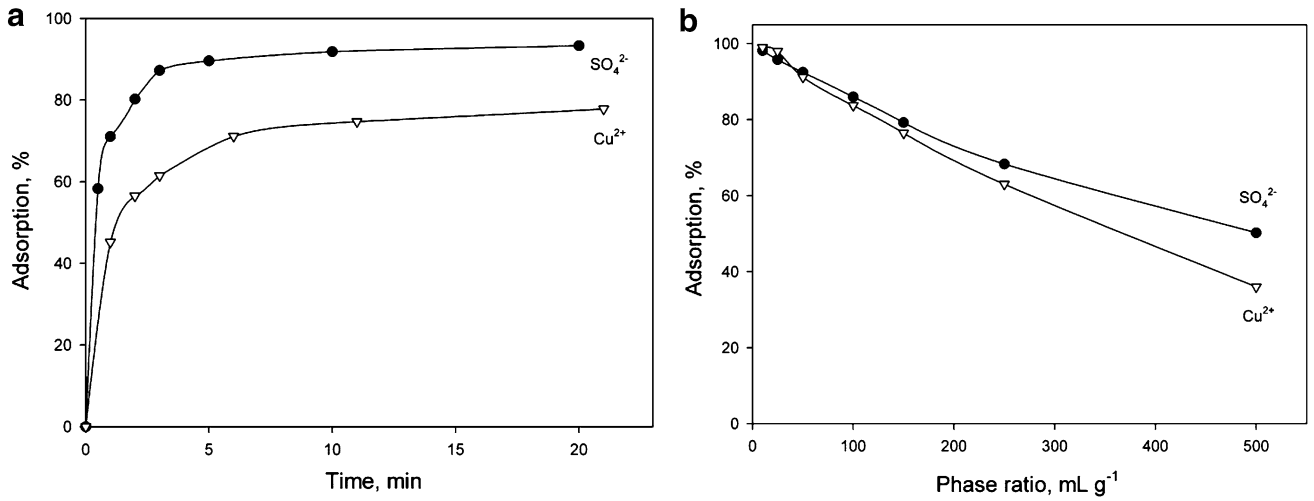

Fig. 6 Dependence of Cu^{2+} and SO_4^{2-} adsorption on MSDN (0.2 g) on time (**a**), and on phase ratio (**b**). **a** obtained with 10 mL of 0.0625 mM $CuSO_4$ in 0.05 M sodium phosphate buffer (pH 5.0) and **b** obtained with 0.625 μmol of $CuSO_4$ in 0.05 M sodium phosphate buffer (pH 5.0)

3.3.2 Kinetics of adsorption

The adsorption kinetics of Cu^{2+} and SO_4^{2-} on MSDN was studied. The maximum of adsorption was achieved after 5 min of shaking and the obtained curves show typical first order adsorption kinetics (Fig. 6a). MSDN demonstrates relatively fast kinetics of adsorption due to dominance of electrostatic interactions as compared with the other types of microporous and mesoporous carbonaceous adsorbents (Chen and Lin 2001). Figure 6b presents the results on adsorption of 0.625 μmol of Cu^{2+} and SO_4^{2-} on 0.2 g of MSDN from continuously increasing volumes of phosphate buffer at pH 5. The calculated distribution constant (K_D) for Cu^{2+} was equal to 280 mL g^{-1}, which is comparable with the K_D values obtained for the carboxylic cation exchangers (Hubicki and Kolodynska 2015).

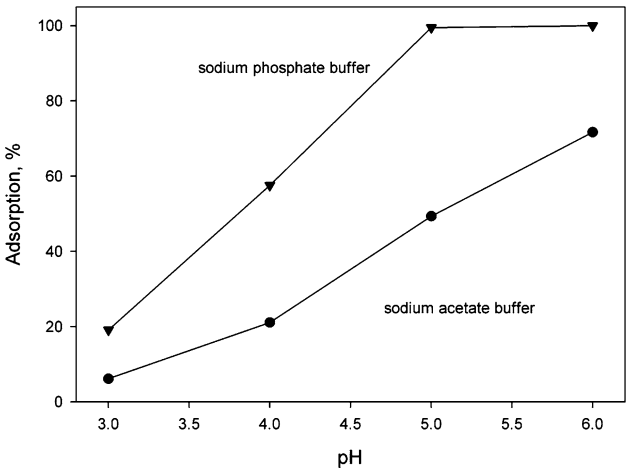

Fig. 7 Adsorption of Cu^{2+} on MSDN (0.2 g) depending on the pH of sodium phosphate and sodium acetate buffers. Experiments were done from 10 mL of 10 μg mL^{-1} Cu^{2+} solution in 0.05 M buffer

3.3.3 The effect of anions on adsorption of copper

As discussed in Sect. 1, MSDN can possess both cation and anion exchange properties. On this reason, the adsorption of anions and cations at different pH can be dependent on each other as proposed by Dolenko et al. (2014). To investigate this option, the effect of anionic component from pH buffers on adsorption of Cu^{2+} was studied. The corresponding dependences obtained for sodium acetate and sodium phosphate buffers are shown in Fig. 7. The

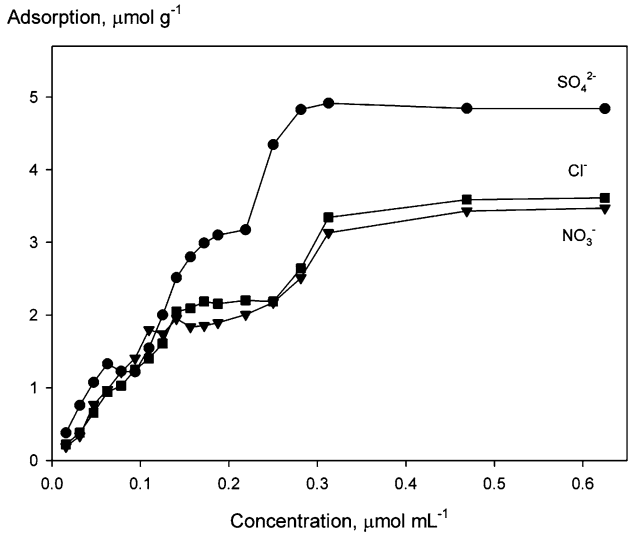

Fig. 8 Adsorption isotherms for Cu^{2+} on MSDN (0.2 g) obtained with 10 mL of Cu^{2+} containing solutions of different salts

adsorption of Cu^{2+} on MSDN occurred at pH >3.0 in both buffers and increased with pH growth. The complete adsorption of Cu^{2+} was achieved from phosphate buffer at pH 5.0, but only partial adsorption of Cu^{2+} was obtained from acetate buffer even at higher pH 6.0. Therefore, this happens due to a stronger adsorption of phosphate, that resulted in increase of negative charge for MSND surface. The adsorbed phosphate acts as an additional adsorption site for metal cations. Another reason for the observed effect is connected with an ability of acetate to form neutral copper acetate complexes [log K = 3.4; (Martell and Smith 2004)] that competes to interaction of Cu^{2+} with carboxyl groups at the surface of MSDN. It should be noted that strong interaction between organophosphonates and hydroxylated diamond surface has been previously used for functionalisation of diamond electrodes (Caterino et al. 2014).

The concentration of ions in pH buffers is significantly higher than the concentration of the analyte; hence, the effect of anions on the adsorption of Cu^{2+} is expected. However, the study of Cu^{2+} adsorption on MSDN from solutions of different copper salts in absence of pH buffers can illustrate better the role of anions. Figure 8 presents the corresponding adsorption isotherms obtained with the solutions of copper chloride, nitrate and sulphate salts. All isotherms have three distinctive "steps", but adsorption of Cu^{2+} from copper sulphate solution was higher than from solutions of corresponding chloride and nitrate salts. The presence of several "steps" in the isotherms is quite unusual and indicates the occurrence of several types of interactions around Cu^{2+} in the system. Since the type of anion does not influence the position of "step", the corresponding interactions must take place at different adsorption sites in MSDN. It should be noted that adsorption isotherms for heavy metals on graphite adsorbents show only one type of adsorption site (Seco et al. 1999) indicating a substantial difference between adsorption properties of graphite and MSDN, despite the presence of thin sp^2 carbon layer at the DND surface (Aleksenskii et al. 1999).

A possible explanation for the observed steps on the adsorption isotherms can be derived from the ζ-potential–pH dependence for MSDN (see Fig. 4). The pH of native

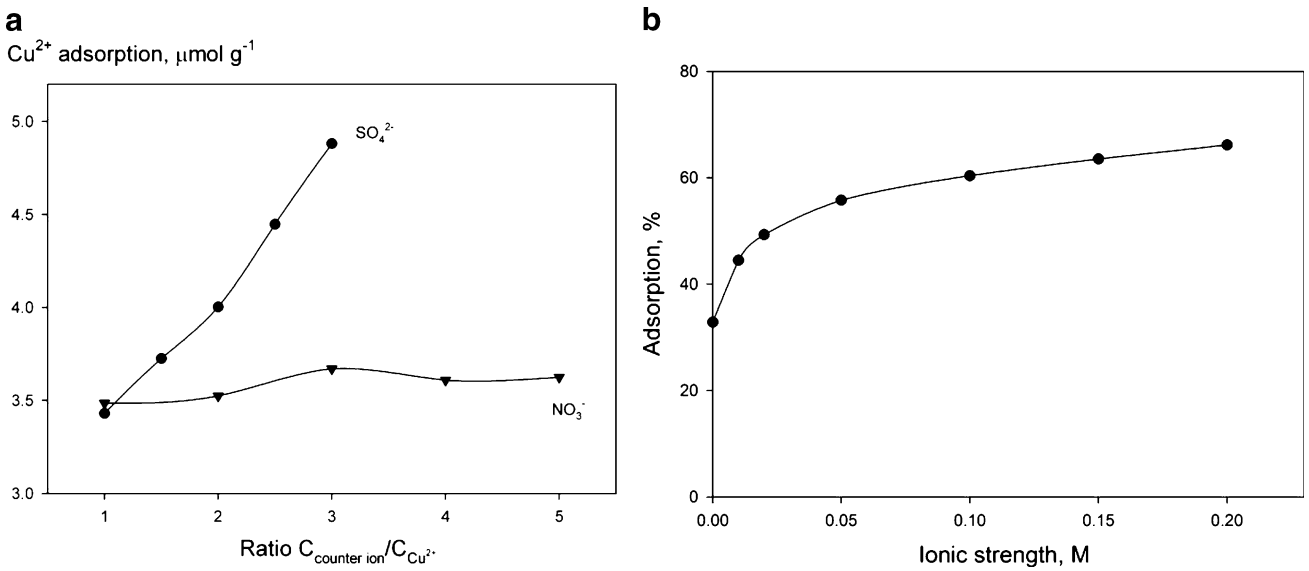

Fig. 9 Influence of nature of anion (**a**) and ionic strength (**b**) on Cu^{2+} adsorption on MSDN (0.2 g). 10 mL of 10 μg mL^{-1} Cu^{2+} solution were used. **a** Na_2SO_4 or $NaNO_3$ were added to increase counter ion/Cu^{2+} ratio. **b** Ionic strength was maintained with $NaNO_3$

MSDN suspension in water is about 4.5–5.0, that means that the surface is positively (+14 mV) charged, and Cu^{2+} adsorption is reduced due to electrostatic repulsion at these conditions. At the same time, counter ions (SO_4^{2-}, NO_3^-, and Cl^-) are adsorbed at this pH and neutralise the surface charge of MSDN, while for doubly charged SO_4^{2-} counter ion it happens at lower concentrations than for the singly charged Cl^- or NO_3^-. Thus, the interaction of MSDN with anions provides an additional step on adsorption isotherm and lead to the higher Cu^{2+} adsorption capacity in the case of $CuSO_4$, as compared to $CuCl_2$ and $Cu(NO_3)_2$. Maximum adsorption capacity was found to be 5 μmol g^{-1} for $CuSO_4$ and 3.5 μmol g^{-1} for $CuCl_2$ and $Cu(NO_3)_2$. To confirm the proposed mechanism the adsorption of Cu^{2+} was additionally investigated from solutions of copper sulphate and copper nitrate with added sodium sulphate and sodium nitrate, respectively. Figure 9a shows the growth in adsorption of Cu^{2+} on MSDN with increase of SO_4^{2-} concentration in the solution, but steady low adsorption with varied concentration of NO_3^-. Therefore, the adsorbed SO_4^{2-} ions can act as an additional adsorption sites for Cu^{2+}.

The ionic strength of the solution influences the adsorption of Cu^{2+} too. As shown in Fig. 9b the adsorption of Cu^{2+} is notably growing with increase of ionic strength, especially in the range of 0–0.05 M. This indicates the suppression of electrostatic repulsion between Cu^{2+} and positively charged MSDN surface, which results in elevated adsorption of Cu^{2+} from concentrated solution of sodium nitrate due to chelation mechanism. This effect is well described for complexing ion-exchangers in the literature (Nesterenko and Jones 2007).

3.4 Adsorption of anions

As counter ions have influence on the metal cation adsorption on MSDN, the adsorption of inorganic anions was carefully studied. Figure 10 shows adsorption isotherms for eight inorganic anions on MSDN and calculated values of distribution coefficients (K_D) as well as an approximation of adsorption isotherms to Langmuir and Freundlich models (Eqs. 2 and 3) are presented in Table 2. The obtained data show that the adsorption of anions is better described by the Langmuir equation except of PO_4^{3-}, which behaviour will be explained later. This is in an agreement with assumption of monolayer adsorption of anions on the MSDN surface. The maximum adsorption capacities for anions vary from 50 to 150 μmol g^{-1}, which are significantly higher than the values obtained for cations. This is the first time when superior anion adsorption capacities are revealed for DND.

The following selectivity order $CH_3COO^- < Cl^- < B_4O_7^{2-} < ClO_4^- < I^- < SO_4^{2-} < C_2O_4^{2-}$ is obtained for

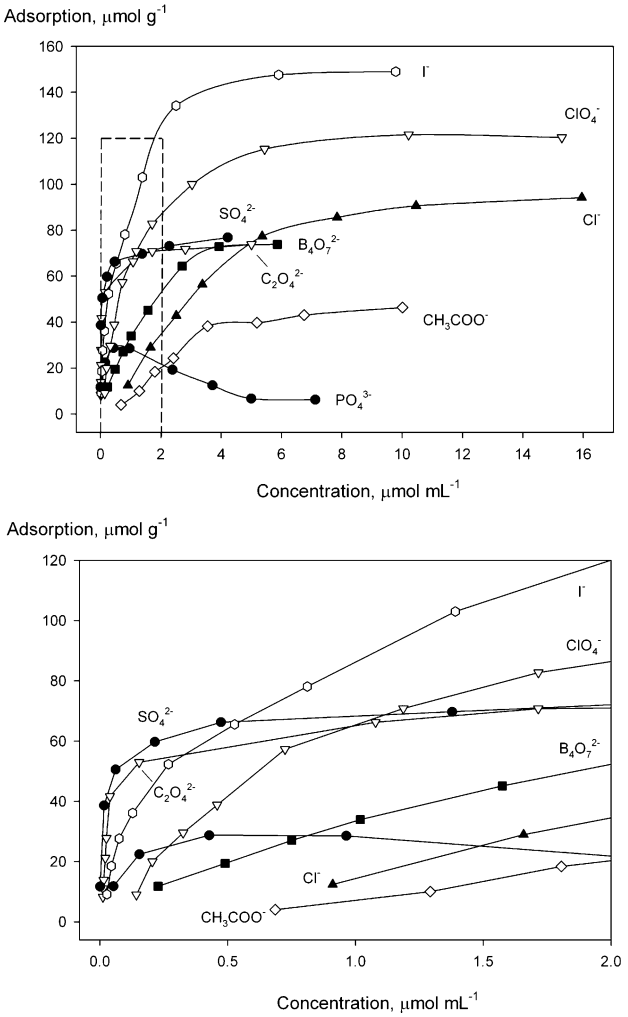

Fig. 10 Isotherms of adsorption on MSDN for eight inorganic anions from 5 mL solutions of sodium salts of increasing concentration. (*bottom figure* gives a magnified view in the area of low initial concentration of anions)

adsorption of anions on MSDN. This sequence is different from common anion-exchange selectivity series $B_4O_7^{2-} < CH_3COO^- < Cl^- < I^- < C_2O_4^{2-} < SO_4^{2-} < ClO_4^-$ known for common anion-exchangers resins with quaternary ammonium and tertiary amino- functional groups (Haddad et al. 2008). MSDN possesses a higher affinity towards $B_4O_7^{2-}$ and $C_2O_4^{2-}$ and lower affinity for ClO_4^-, which means that the presence of not only ion-exchange adsorption mechanisms for this adsorbent. For example, FTIR spectrum (Fig. 3) shows the presence of high concentration of hydroxyl groups at the surface of MSDN particles, which can form polyol complexes with $B_4O_7^{2-}$ (Simonnot et al. 2000). Also, ICP-MS analysis of purified MSDN confirms the presence of significant amount of metal impurities (Mitev et al. 2013), such as Ca^{2+}, Sr^{2+} and Ba^{2+}, which contribute into adsorption of $C_2O_4^{2-}$ or PO_4^{3-}.

Table 2 Adsorption capacity and distribution coefficients for anion adsorption on MSDN and adsorption modelling with Langmuir and Freundlich equations

Anion	Experiment		Langmuir model (Eq. 2)			Freundlich model (Eq. 3)		
	K_D (mL g^{-1})	A_{max} (μmol g^{-1})	R^2	K_L (mL μmol^{-1})	A_{max} (μmol g^{-1})	R^2	n	K_F
$C_2O_4^{2-}$	870 ± 70	74 ± 2	0.988	21.0 ± 2.0	73 ± 4	0.930	4.5 ± 0.7	58 ± 9
$B_4O_7^{2-}$	45 ± 3	74 ± 2	0.994	0.50 ± 0.05	104 ± 5	0.974	2.0 ± 0.3	34 ± 5
CH_3COO^-	10 ± 1	47 ± 1	0.971	0.20 ± 0.02	75 ± 4	0.937	1.73 ± 0.30	14 ± 2
Cl^-	17 ± 2	95 ± 2	0.985	0.21 ± 0.02	131 ± 6	0.943	2.12 ± 0.30	29 ± 4
I^-	325 ± 21	150 ± 4	0.992	1.55 ± 0.16	160 ± 8	0.970	3.11 ± 0.50	81 ± 12
SO_4^{2-}	552 ± 44	77 ± 2	0.979	59.0 ± 6.0	71 ± 4	0.963	7.3 ± 1.1	67 ± 10
ClO_4^-	90 ± 8	121 ± 3	0.998	0.94 ± 0.10	134 ± 6	0.941	3.10 ± 0.50	58 ± 9

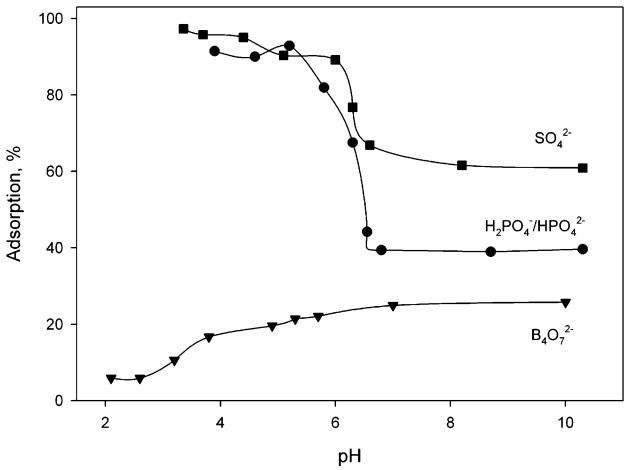

Fig. 11 pH influence on phosphate, sulphate and borate adsorption on MSDN (0.2 g) from 10 mL of 100 μmol mL^{-1} solution. NaOH/HNO_3 was used to adjust pH and ionic strength (μ = 0.01 M)

The shape of adsorption isotherm for PO_4^{3-} (see Fig. 10) differs from that observed for other anions. Its part obtained for low anion concentrations matches the adsorption isotherms obtained for the other anions, but with further increase of phosphate concentration in solution the adsorption suddenly decreases and remains at very low level. A possible explanation for this behaviour is that both the MSDN suspension and Na_3PO_4 solution used in this experiment have pH buffering capacity around pH of ~5 and 12, respectively. Therefore, at low Na_3PO_4 concentrations the pH of the system is defined by the pK_a of MSDN particles and is equal to ~5. It means a positively charged (see Fig. 4) surface of MSDN particles which provides adsorption of phosphate as has been reported by Caterino et al. (2014). However, a further increase in the concentration of Na_3PO_4 causes a substantial rise in pH due to strong basicity of PO_4^{3-} and switches the ζ-potential to negative values. Correspondingly, the adsorption of phosphate decreases due to raising electrostatic repulsion from the MSDN surface. A strong influence of PO_4^{3-} concentration on the ζ-potential of nanodiamond was also confirmed in work of Zhu et al. (2004). The described effect was not observed for other anions as they have no buffering capacity at high pHs, except of $B_4O_7^{2-}$. However, the adsorption mechanism for $B_4O_7^{2-}$ is different and related to the complexation with diol groups. In this case, increase of pH provides higher adsorption values as stability of $B_4O_7^{2-}$–diol complexes is growing with pH (Simonnot et al. 2000). To confirm the hypotheses the dependence of adsorption on pH of the solutions was obtained for borate, sulphate and phosphate (see Fig. 11). The concentration of solutes was kept constant and pH of the solutions was adjusted by addition of small volumes of concentrated HNO_3 or NaOH. For $H_2PO_4^-$ and SO_4^{2-} a remarkable drop in adsorption is observed at pH 7, which is close to the isoelectric point for MSDN. Obviously, it follows to sharp decrease in electrostatic attraction for these anions, while the adsorption of $B_4O_7^{2-}$ gradually grows with pH increase.

The kinetics of adsorption of SO_4^{2-} is similar to that discussed before for Cu^{2+} (Fig. 6a), when adsorption equilibrium can be reached in 10–20 min. K_D value 563 ± 16 mL g^{-1} calculated for adsorption of SO_4^{2-} from diluted solutions (Fig. 6b) is consistent with the value obtained from the SO_4^{2-} adsorption isotherm (552 ± 44 mL g^{-1}, see Table 2).

4 Conclusions

The adsorption of di- and tri-valent metals cations and inorganic anions from aqueous solutions on MSDN is investigated. For the first time for DND based material, the significantly higher adsorption capacities (50–150 μmol g^{-1}) are obtained for anions as compared with adsorption capacities (<9 μmol g^{-1}) calculated for cations. It is shown that adsorption of anions is mainly due to electrostatic ion-exchange interactions, while adsorption of cation is mainly due to complexation with carboxyl- and hydroxyl-functional groups at the surface of MSDN. The specific or

chemisorption type of interactions are noted for adsorption of borate and attributed to the formation of borate–polyol type of complexes with hydroxyl groups at the surface of MSDN. Interactions with metal impurities can impact in the adsorption SO_4^{2-} and $C_2O_4^{2-}$. The effect of conjoint type of simultaneous adsorption of metal cations and doubly and triply charged anions is also observed. Adsorption of ions on the MSDN surface obeys Langmuir law. The distribution coefficients for the calculated for adsorption of anions on MSDN are ranging between 10 and 870 mL g^{-1}.

Acknowledgments This work was supported by grants from the Australian Research Council to ACROSS (DP110102046 and DP150101518). The authors would also like to acknowledge the Central Science Laboratory (University of Tasmania) and for substantial instrumental support and service.

References

Aleksenskii, A.E., Baidakova, M.V., Vul', A.Y., Siklitskii, V.I.: The structure of diamond nanoclusters. Phys. Solid State **41**, 668–671 (1999)

Boehm, H.P.: Some aspects of the surface-chemistry of carbon-blacks and other carbons. Carbon **32**, 759–769 (1994)

Bogatyreva, G.P., Marinich, M.A., Gvyazdovskaya, V.L.: Diamond—an adsorbent of a new type. Diam. Relat. Mater. **9**, 2002–2005 (2000)

Bogatyreva, G.P., Marinich, M.A., Bazalii, G.A., Gvyazdovskaya, V.L.: Polycrystalline nanodiamond based powders as adsorbents for biological media. Nanosyst. Nanomater. Nanotechnol. **6**, 1227–1236 (2008a)

Bogatyreva, G.P., Voloshin, M.N., Padalko, V.I.: Detonation synthesized nanodiamond powder for the preparation of porous polycrystalline micron powders. Diam. Relat. Mater. **17**, 213–216 (2008b)

Bogatyreva, G.P., Marinich, M.A., Bazalii, G.A.: Application of nanocarbon materials for the purification of biological media. Electron. Comm. **15**, 34–38 (2010a). http://elc.kpi.ua/issue/archive

Bogatyreva, G.P., Marinich, M.A., Bazalii, G.A., Il'niskaya, G.D.: Adsorption processes on the surface of new types of diamond powders in biological media. Nanosyst. Nanomater. Nanotechnol. **8**, 851–859 (2010b)

Buchatskaya, Y., Romanchuk, A., Yakovlev, R., Shiryaev, A., Kulakova, I., Kalmykov, S.: Sorption of actinides onto nanodiamonds. Radiochim. Acta **103**, 205–211 (2015)

Caterino, R., Csiki, R., Wiesinger, M., Sachsenhauser, M., Stutzmann, M., Garrido, J.A., Cattani-Scholz, A., Speranza, G., Janssens, S.D., Haenen, K.: Organophosphonate biofunctionalization of diamond electrodes. ACS Appl. Mater. Interf. **6**, 13909–13916 (2014)

Chang, L.Y., Osawa, E., Barnard, A.S.: Confirmation of the electrostatic self-assembly of nanodiamonds. Nanoscale **3**, 958–962 (2011)

Chen, J.P., Lin, M.S.: Equilibrium and kinetics of metal ion adsorption onto a commercial H-type granular activated carbon: experimental and modeling studies. Water Res. **35**, 2385–2394 (2001)

Chen, W.H., Lee, S.C., Sabu, S., Fang, H.C., Chung, S.C., Han, C.C., Chang, H.C.: Solid-phase extraction and elution on diamond (SPEED): a fast and general platform for proteome analysis with mass spectrometry. Anal. Chem. **78**, 4228–4234 (2006)

Chiganova, G.A., Bondar, V.A., Chiganov, A.S.: Electrophoretic behavior of hydrosols of ultradisperse diamond and modification of its surface. Colloid J. Russ. Acad. Sci. **55**, 774–775 (1993)

Chiganova, G.A., Chul'myakova, D.A., Mordvinova, L.E., Petrova, T.I.: A nickel-substituted form of nanodiamonds and its catalytic activity in decomposition of hydrogen peroxide. Russ. J. Appl. Chem. **85**, 177–181 (2012)

Chiganova, G.A., Tyryshkina, L.E., Ivanenko, A.A.: Nanodiamonds effect on characteristics of copper galvanic coatings. Russ. J. Appl. Chem. **86**, 1311–1313 (2013)

Chukhaeva, S.I., Cheburina, L.A.: Sorption activity of nanodiamonds on cesium. Sverkhtv. Mater. **2**, 43–48 (2000)

Dolenko, T.A., Burikov, S.A., Laptinskiy, K.A., Laptinskaya, T.V., Rosenholm, J.M., Shiryaev, A.A., Sabirov, A.R., Vlasov, I.I.: Study of adsorption properties of functionalized nanodiamonds in aqueous solutions of metal salts using optical spectroscopy. J. Alloys Compd. **586**, S436–S439 (2014)

Fedyanina, O.N., Nesterenko, P.N.: Regularities of chromatographic retention of phenols on microdispersed sintered detonation nanodiamond in aqueous-organic solvents. Russ. J. Phys. Chem. A **84**, 476–480 (2010)

Fedyanina, O.N., Nesterenko, P.N.: Regularities of retention of benzoic acids on microdispersed detonation nanodiamonds in water-methanol mobile phases. Russ. J. Phys. Chem. A **85**, 1773–1777 (2011)

Gibson, N., Shenderova, O., Luo, T.J.M., Moseenkov, S., Bondar, V., Puzyr, A., Purtov, K., Fitzgerald, Z., Brenner, D.W.: Colloidal stability of modified nanodiamond particles. Diam. Relat. Mater. **18**, 620–626 (2009)

Goertzen, S.L., Theriault, K.D., Oickle, A.M., Tarasuk, A.C., Andreas, H.A.: Standardization of the Boehm titration. Part I. CO_2 expulsion and endpoint determination. Carbon **48**, 1252–1261 (2010)

Haddad, P.R., Nesterenko, P.N., Buchberger, W.: Recent developments and emerging directions in ion chromatography. J. Chromatogr. A **1184**, 456–473 (2008)

Hubicki, Z., Kolodynska, D.: Selective Removal of Heavy Metal Ions from Waters and Waste Waters Using Ion Exchange Methods. InTech, Rijeka (2015)

Hunter, R.J.: Zeta Potential in Colloid Science: Principles and Applications. Academic Press, London (1981)

Ivanov, M.G., Pavlyshko, S.V., Ivanov, D.M., Petrov, I., Shenderova, O.: Synergistic compositions of colloidal nanodiamond as lubricant-additive. J. Vac. Sci. Technol. B **28**, 869–877 (2010)

Kalijadis, A.M., Vukcevic, M.M., Jovanovic, Z.M., Lausevic, Z.V., Lausevic, M.D.: Characterisation of surface oxygen groups on different carbon materials by the Boehm method and temperature-programmed desorption. J. Serb. Chem. Soc. **76**, 757–768 (2011)

Kulakova, I.I.: Surface chemistry of nanodiamonds. Phys. Solid State **46**, 636–643 (2004)

Manus, L.M., Mastarone, D.J., Waters, E.A., Zhang, X.Q., Schultz-Sikma, E.A., MacRenaris, K.W., Ho, D., Meade, T.J.: Gd(III)–nanodiamond conjugates for MRI contrast enhancement. Nano Lett. **10**, 484–489 (2010)

Martell AE, Smith RM (2004) NIST critically selected stability constants of metal complexes. NIST standard reference database 46. Version 8.0

Mitev, D.P., Townsend, A.T., Paull, B., Nesterenko, P.N.: Direct sector field ICP-MS determination of metal impurities in detonation nanodiamond. Carbon **60**, 326–334 (2013)

Mitev, D.P., Townsend, A.T., Paull, B., Nesterenko, P.N.: Microwave-assisted purification of detonation nanodiamond. Diam. Relat. Mater. **48**, 37–46 (2014a)

Mitev, D., Townsend, A., Paull, B., Nesterenko, P.: Screening of elemental impurities in commercial detonation nanodiamond using sector field inductively coupled plasma-mass spectrometry. J. Mater. Sci. **49**, 3573–3591 (2014b)

Mochalin, V.N., Shenderova, O., Ho, D., Gogotsi, Y.: The properties and applications of nanodiamonds. Nat. Nanotechnol. **7**, 11–23 (2012)

Nesterenko, P.N., Fedyanina, O.N.: Properties of microdispersed sintered nanodiamonds as a stationary phase for normal-phase high performance liquid chromatography. J. Chromatogr. A **1217**, 498–505 (2010)

Nesterenko, P.N., Haddad, P.R.: Diamond-related materials as potential new media in separation science. Anal. Bioanal. Chem. **396**, 205–211 (2010)

Nesterenko, P.N., Jones, P.: Recent developments in the high-performance chelation ion chromatography of trace metals. J. Sep. Sci. **30**, 1773–1793 (2007)

Nesterenko, P.N., Fedyanina, O.N., Volgin, Y.V., Jones, P.: Ion chromatographic investigation of ion-exchange properties of microdisperse sintered nanodiamonds. J. Chromatogr. A **1155**, 2–7 (2007)

Nguyen, T.T.B., Chang, H.C., Wu, V.W.K.: Adsorption and hydrolytic activity of lysozyme on diamond nanocrystallites. Diam. Relat. Mater. **16**, 872–876 (2007)

Ozawa, M., Inaguma, M., Takahashi, M., Kataoka, F., Kruger, A., Osawa, E.: Preparation and behavior of brownish, clear nanodiamond colloids. Adv. Mater. **19**, 1201–1206 (2007)

Paci, J.T., Man, H.B., Saha, B., Ho, D., Schatz, G.C.: Understanding the surfaces of nanodiamonds. J. Phys. Chem. C **117**, 17256–17267 (2013)

Penner, N.A., Nesterenko, P.N.: Application of neutral hydrophobic hypercrosslinked polystyrene to the separation of inorganic anions by ion chromatography. J. Chromatogr. A **884**, 41–51 (2000)

Peristyy, A.A., Fedyanina, O.N., Paull, B., Nesterenko, P.N.: Diamond based adsorbents and their application in chromatography. J. Chromatogr. A **1357**, 68–86 (2014)

Peristyy, A., Paull, B., Nesterenko, P.N.: Chromatographic performance of synthetic polycrystalline diamond as a stationary phase in normal phase high performance liquid chromatography. J. Chromatogr. A **1391**, 49–59 (2015)

Petit, T., Girard, H.A., Trouve, A., Batonneau-Gener, I., Bergonzo, P., Arnault, J.C.: Surface transfer doping can mediate both colloidal stability and self-assembly of nanodiamonds. Nanoscale **5**, 8958–8962 (2013)

Sakurai, H., Ebihara, N., Osawa, E., Takahashi, M., Fujinami, M., Oguma, K.: Adsorption characteristics of a nanodiamond for oxoacid anions and their application to the selective preconcentration of tungstate in water samples. Anal. Sci. **22**, 357–362 (2006)

Schmidlin, L., Pichot, V., Comet, M., Josset, S., Rabu, P., Spitzer, D.: Identification, quantification and modification of detonation nanodiamond functional groups. Diam. Relat. Mater. **22**, 113–117 (2012)

Seco, A., Gabaldon, C., Marzal, P., Aucejo, A.: Effect of pH, cation concentration and sorbent concentration on cadmium and copper removal by a granular activated carbon. J. Chem. Technol. Biotechnol. **74**, 911–918 (1999)

Shames, A.I., Panich, A.M., Osipov, V.Y., Aleksenskiy, A.E., Vul', A.Y., Enoki, T., Takai, K.: Structure and magnetic properties of detonation nanodiamond chemically modified by copper. J. Appl. Phys. **107**, 014318 (2010)

Simonnot, M.O., Castel, C., Nicolai, M., Rosin, C., Sardin, M., Jauffret, H.: Boron removal from drinking water with a boron selective resin: is the treatment really selective? Water Res. **34**, 109–116 (2000)

Skorik, N.A., Krivozubov, A.L., Karzhenevskii, A.P., Spitsyn, B.V.: Physicochemical study of the nanodiamond surface. Prot. Met. Phys. Chem. Surf. **47**, 54–58 (2011)

Strelko, V., Malik, D.J.: Characterization and metal sorptive properties of oxidized active carbon. J. Colloid Interf. Sci. **250**, 213–220 (2002)

Watanabe, M., Kimura, T.: Adsorption of actinides on diamond surface. International Conference on Diamond and Carbon Materials, Granada, Spain O81 (2012)

Wiest, L.A., Jensen, D.S., Hung, C.H., Olsen, R.E., Davis, R.C., Vail, M.A., Dadson, A.E., Nesterenko, P.N., Linford, M.R.: Pellicular particles with spherical carbon cores and porous nanodiamond/polymer shells for reversed-phase HPLC. Anal. Chem. **83**, 5488–5501 (2011)

Williams, O.A.: Nanocrystalline diamond. Diam. Relat. Mater. **20**, 621–640 (2011)

Yushin, G.N., Osswald, S., Padalko, V.I., Bogatyreva, G.P., Gogotsi, Y.: Effect of sintering on structure of nanodiamond. Diam. Relat. Mater. **14**, 1721–1729 (2005)

Zhu, Y.W., Shen, X.Q., Feng, Z.J., Xu, X.G., Wang, B.C.: On the zeta-potential of nanodiamond in aqueous systems. J. Mater. Sci. Technol. **20**, 469–471 (2004)

Zhu, Y., Li, W., Zhang, Y., Li, J., Liang, L., Zhang, X., Chen, N., Sun, Y., Chen, W., Tai, R., Fan, C., Huang, Q.: Excessive sodium ions delivered into cells by nanodiamonds: implications for tumor therapy. Small **8**, 1771–1779 (2012)

Zhu, Y., Zhang, Y., Shi, G., Yang, J., Zhang, J., Li, W., Li, A., Tai, R., Fang, H., Fan, C., Huang, Q.: Nanodiamonds act as Trojan horse for intracellular delivery of metal ions to trigger cytotoxicity. Part. Fibre Toxicol. **12**, 1–11 (2015)